

Structural study of Rb and Cl coadsorption on Cu(111): a case of overlayer compound formation

This article has been downloaded from IOPscience. Please scroll down to see the full text article.

1997 J. Phys.: Condens. Matter 9 4593

(<http://iopscience.iop.org/0953-8984/9/22/011>)

View [the table of contents for this issue](#), or go to the [journal homepage](#) for more

Download details:

IP Address: 171.66.16.207

The article was downloaded on 14/05/2010 at 08:49

Please note that [terms and conditions apply](#).

Structural study of Rb and Cl coadsorption on Cu(111): a case of overlayer compound formation

J Lüdecke†, S Skordas‡, G J Jackson†, D P Woodruff†, R G Jones§,
B C C Cowie||, R Ithnin§ and C A Papageorgopoulos‡

† Physics Department, University of Warwick, Coventry CV4 7AL, UK

‡ Physics Department, University of Ioannina, PO Box 1186, Ioannina, 451 10, Greece

§ Department of Chemistry, University of Nottingham, Nottingham NG7 2RD, UK

|| CCLRL Daresbury Laboratory, Warrington WA4 4AD, UK

Received 12 February 1997

Abstract. A structural study of the adsorption of Rb on a Cu(111)($\sqrt{3} \times \sqrt{3}$)R30°-Cl surface has been conducted using normal-incidence x-ray standing-wavefield absorption at both the Cl and Rb surface atoms. The results indicate reaction of the coadsorbates to form an overlayer of approximately 1.2 ML of RbCl(100) which is essentially incommensurate with the substrate. The RbCl–Cu outermost layer spacing is similar to that seen for pure Rb adsorption on Cu(111). This RbCl layer is spread over the surface and not agglomerated into thicker islands. The results are consistent with prior characterization of the system by Auger electron spectroscopy and temperature-programmed desorption, and with STM studies of NaCl deposition on Al(111).

1. Introduction

Coadsorption studies in surface science are an important step in understanding the reactivity of surfaces and are of particular relevance to heterogeneous catalysis. Despite the key role of structure in many such processes, there are still rather few quantitative structural studies of coadsorption systems, although this deficiency is being slowly addressed by a range of methods. In this paper we report on the results of an investigation of a coadsorption structure formed by Rb and Cl on Cu(111), using the technique of normal-incidence x-ray standing-wavefield absorption (NIXSW). In such a system, involving coadsorption of highly electropositive and electronegative species, we might expect one of two possible consequences. The first is that both species chemisorb to the substrate but interact either through direct charge transfer or via a through-metal coupling, to produce some form of structural modification relative to the geometry adopted by the individual species on the same surface. For example, alkali metal atoms show effective radii variations of up to about 1 Å depending on whether their bonding environment is highly ionic or metallic. A second possibility is that the interaction of the coadsorbates is stronger than their interaction with the substrate, and that surface compound formation occurs. Although there have been extensive studies of the influence of the role of adsorbed alkali metals on molecular dissociation and reaction rates (e.g. [1]) and a few related structural studies, notably of CO/alkali [2–4] and O/alkali [5–7] coadsorption, there appear to be few studies of alkali and halogen coadsorption. Some exceptions include K/Cl coadsorption on Ag(100) [8], RbCl deposition on Si(100) and W(110) [9], Na/Br coadsorption on WSe₂(0001) [10] and Cs/Cl coadsorption on Si(100) [11]. None of these are full structural studies, but in most

cases indications of individual substrate bonding or alkali halide compound formation could be inferred indirectly. In the case of the Ag(100) substrate the situation is complicated by the tendency to form AgCl, but under certain regimes of temperature and relative coverage, KCl formation was believed to occur. Perhaps most relevant is the RbCl adsorption work which was interpreted in terms of compound formation only for coverages greater than 0.4 ML. While NaBr formation was also found on WSe₂ at higher coverages with room temperature annealing, CsCl formation was not considered in the final example on Si(100).

Our results indicate that in the Rb/Cl/Cu(111) case, surface compound formation does occur at nominal coverages of 0.33 ML. This conclusion is consistent with prior characterization of the system [12], most notably by temperature-programmed desorption, which shows concerted desorption of the coadsorbates at a temperature not corresponding to desorption of either species in the absence of coadsorption. Our conclusions regarding the structure of the surface compound, a thinly spread layer of RbCl(100) of nominal thickness about 1.2 ML, but with no evidence for thicker island formation, is also very similar to the results of a recent STM study of NaCl deposition on Al(111) [13].

2. Experimental details and results

The experiments were conducted on beamline 6.3 of the Synchrotron Radiation Source (SRS) at the Daresbury Laboratory of the CLRC (Central Laboratories for the Research Councils); this station is equipped with a grazing incidence toroidal pre-focusing mirror, an ultrahigh-vacuum double-crystal monochromator, and a surface spectrometer end-station [14, 15]. The latter is fitted with LEED optics to allow *in situ* characterization of the degree of surface order, and a VSW HA100 concentric hemispherical electrostatic electron energy analyser which was used to detect the photoelectrons and Auger electron emission from the sample resulting from the incident x-radiation. A double-pass cylindrical mirror analyser with integral electron gun was also used to characterize the surface cleanliness using Auger electron spectroscopy. The Cu(111) sample was prepared by the usual combination of x-ray Laue alignment, spark machining, mechanical polishing, and *in situ* argon-ion bombardment and annealing cycles until a clean and well-ordered sample was obtained as judged by Auger electron spectroscopy and LEED. The specific Rb/Cl coadsorption system studied here was obtained by first forming the Cu(111)($\sqrt{3} \times \sqrt{3}$)R30°-Cl surface phase and then exposing this to Rb from a well-outgassed SAES getter source. Prior work which we have performed on Cl adsorption on Cu(111), both in the initial NIXSW study of this system [16, 17], and in characterization of the general characteristics of Rb/Cl coadsorption on Cu(111) [12], was conducted using a solid-state electrochemical source of Cl₂ in the UHV chamber. In the present experiment this source failed and instead the initial Cl surface layer was formed by electron-induced decomposition of dichloroethane (ClCH₂CH₂Cl), a reaction which we have previously shown to produce a carbon-free and generally well-ordered surface [18–20]. This was achieved by first dosing the sample with the molecular vapour at 160 K (to a coverage somewhat in excess of 1 ML) and then using the LEED electron gun to dissociate the layer, while monitoring the LEED pattern to follow the process; this resulted in either a ($\sqrt{3} \times \sqrt{3}$) or a ($6\sqrt{3} \times 6\sqrt{3}$) LEED pattern, the latter being associated with the slightly higher-coverage ‘compressed’ phase. Warming to room temperature then caused desorption of all remaining reaction products other than the Cl. If the higher coverage Cl phase was obtained, subsequent heating to sequentially higher temperatures was undertaken to remove the excess Cl and obtain the ($\sqrt{3} \times \sqrt{3}$)R30°-Cl phase. Most of the measurements concentrated on a coadsorption phase formed by exposing this surface to Rb at room temperature to nominal saturation, although some data were also collected from a surface dosed with approximately

one half of this Rb coverage; the lower Rb coverage appeared to lead to a mixed phase structure which thus had a lower average order, and these data are not discussed further. No attempt was made to make LEED measurements on the coadsorbed phase because the prior characterization study had revealed very serious electron-stimulated desorption from this phase [12]. NIXSW measurements were taken with the sample cooled to a nominal temperature of 160 K to reduce the effect of thermal vibrations.

The x-ray standing-wavefield technique exploits the fact that close to the conditions for an x-ray Bragg reflection in a crystal there is a range of photon energy or incidence angle over which the incident and scattered x-rays interfere to form a standing wavefield with a periodicity equal to that of the scatterer planes and a phase which is a well-understood function of the photon energy. A study of the x-ray absorption in an adsorbate species through the Bragg condition leads to an absorption profile which is characteristic of the location of the adsorbate atom relative to the extended bulk scatterer planes. By making such measurements relative to two or more different scatterer plane orientations, one can obtain the adsorbate location in real space by a simple triangulation of the layer spacings in different directions. The NIXSW variant of the method which we use here [16, 17] exploits the fact that at near-normal incidence to the relevant scatterer planes (which may, or may not, be parallel to the surface) there is no sensitivity to the mosaicity of the substrate crystal, so the method can be used for normal-metal single crystals; by contrast, at a more arbitrary incidence angle the 'rocking curve' width defining the angular range of the high-reflectivity range can be so narrow as to preclude use of all but the most perfect crystals.

The NIXSW data were collected and analysed using similar procedures to those which we have described previously (e.g. [16, 17, 21, 22]). In particular, the sample was first set at normal incidence to the incident x-ray beam, this angle being optimized to achieve the minimum energy of the (111) Bragg reflection and the strongest x-ray reflection peak seen passing back down the beamline to the incident flux monitor. The photon energy was then stepped in 0.2 eV increments through the region of the Bragg condition over a total range of 20 eV, while at each energy step the electron emission intensity was measured sequentially at six different kinetic energies corresponding to Cu LVV and Cl KLV Auger electron peaks, to the Rb 2p photoelectron emission peak, and to kinetic energies 5 eV above each of these. These background signals allowed the corrected intensities of the Cu, Cl and Rb characteristic emission signals to be determined. Simultaneous measurements were made of the total electron yield. A similar set of measurements was made with the crystal turned by 70.5° towards the electron energy analyser in the appropriate $\langle 211 \rangle$ azimuth to excite the $(\bar{1}11)$ Bragg reflection at normal incidence. After normalization to the average values at photon energies away from the Bragg peak, this procedure yielded six XSW absorption profiles characteristic of the Cu, Cl and Rb absorbers in the (111) and $(\bar{1}11)$ x-ray standing waves. Separate measurements were also made of the pure Cu(111)($\sqrt{3} \times \sqrt{3}$)R30°-Cl and Cu(2 × 2)-Rb surface phases; both of these systems have been previously studied by NIXSW [16, 17, 23] but comparative studies provided a valuable reference for the integrity of our data.

The basic structural information contained in the XSW profiles is completely defined by two parameters, the coherent position and the coherent fraction. For a simple single-site geometry, these correspond to the layer spacing of the absorbers relative to the (extended) bulk scatterer planes, and a measure of the degree of order; the coherent fraction in such a case can be related to a Debye-Waller factor describing both the dynamic and static disorder. In more complex situations, the interpretation of these two parameters is less trivial [24], as we discuss in the next section. In addition to these structural parameters, however, fitting the experimental profiles also requires knowledge of two non-structural parameters, namely

the (assumed Gaussian) instrumental energy broadening, and the absolute energy scale. Our procedure is to optimize the fit to the substrate XSW profile assuming a coherent position of zero (absorbers on the scatterer planes) but adjusting the non-structural parameters and the coherent fraction, and then to fit the adsorbate XSW profiles holding the non-structural parameters fixed and changing only the coherent position and fraction of the adsorbate.

Table 1. Fitting parameters obtained from the Cl and Rb XSW absorption profiles recorded from Cl, Rb, and coadsorbed Cl and Rb on Cu(111). Values marked * have one Cu(111) bulk layer spacing added as discussed in the text.

Absorber/phase	Reflection	D (Å)	f_{co}
Cu(111)($\sqrt{3} \times \sqrt{3}$)R30°-Cl			
Cl	(111)	1.81 ± 0.05	0.79 ± 0.05
	($\bar{1}\bar{1}\bar{1}$)	1.96 ± 0.05	0.55 ± 0.05
Cu(111)(2 × 2)-Rb			
Rb	(111)	$2.96 \pm 0.05^*$	0.93 ± 0.05
	($\bar{1}\bar{1}\bar{1}$)	0.90 ± 0.05	0.17 ± 0.10
Cu(111)($\sqrt{3} \times \sqrt{3}$)R30°-Cl + saturation Rb			
Rb	(111)	$2.81 \pm 0.05^*$	0.72 ± 0.10
	($\bar{1}\bar{1}\bar{1}$)	0.87 ± 0.05	0.18 ± 0.10
Cl	(111)	$2.72 \pm 0.05^*$	0.50 ± 0.10
	($\bar{1}\bar{1}\bar{1}$)	1.10 ± 0.05	0.16 ± 0.10

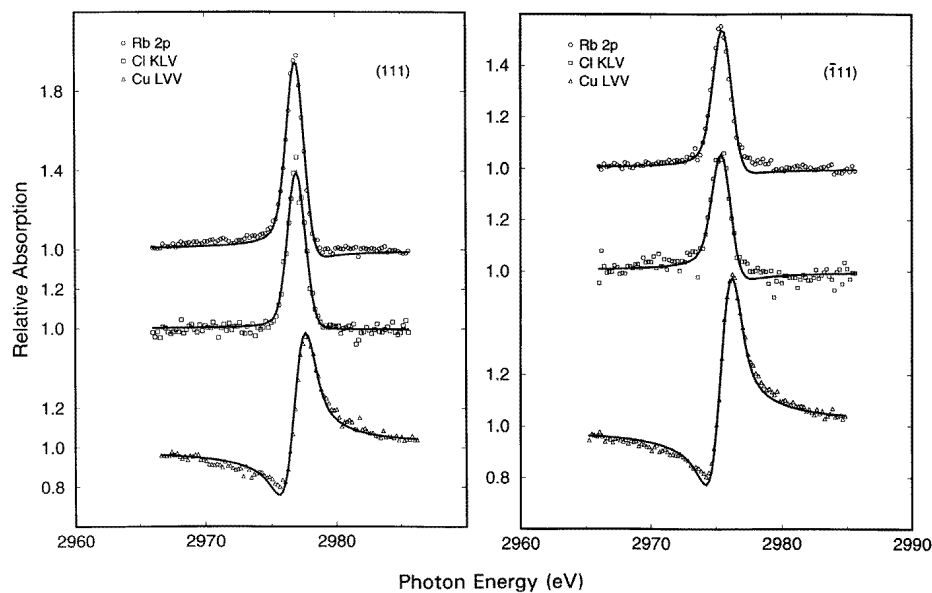


Figure 1. Experimental (symbols) and simulated (full lines) NIXSW absorption profiles at the Cu, Cl and Rb absorbers obtained from the Cl/Rb coadsorption phase on Cu(111). The fitting parameters used in the simulations are given in table 1.

Experimental NIXSW absorption profiles, and the optimized fits, for the coadsorption phase are shown in figure 1, while the fitting parameters for these data and for the measurements on the pure Cl and Rb layers are summarized in table 1. In all cases fits to the Cu NIXSW absorption profiles were consistent with the ideal bulk site positions (to within the precision of the measurements ($\approx \pm 0.05$ Å), which in any case average over several layers) and with coherent fractions in the range 0.89 ± 0.06 .

3. Data interpretation and discussion

The NIXSW data from the pure Cl and Rb phases are in excellent agreement with previously published studies of these systems but a brief discussion of them provides a valuable means of reviewing some of the key features of the technique which will be utilized to discuss the coadsorption data. The simplest structures can be determined using XSW by simple triangulation of the coherent positions, equating these values to layer spacings of single discrete sites. In this interpretation we compare the actual $(\bar{1}11)$ coherent position with the layer spacing expected in this direction on the basis of the measured (111) layer spacing (coherent position), $z(111)$, and the possible high-symmetry adsorption sites. For a bulk layer spacing of $d(111)$ (2.08 Å in the case of Cu(111)) the $z(\bar{1}11)$ values expected for the atop, hcp hollow (above a second-layer Cu atom) and fcc hollow (above a third-layer Cu atom) sites are $z(111)/3$, $(z(111) + d(111))/3$ and $(z(111) + 2d(111))/3$ respectively. For the Cu(111)($\sqrt{3} \times \sqrt{3}$)R30°-Cl phase this leads to the conclusion that Cl occupies fcc hollow sites (the $(\bar{1}11)$ layer spacing predicted from the (111) measurements is 1.99 Å, in good agreement with the experimental value) while in Cu(111)(2 × 2)-Rb the Rb coherent positions are consistent with atop site occupation (the predicted value of 0.99 Å is also close to the measured value). Note that in the case of the Rb(111) coherent position, the value given is the experimental value plus one bulk layer spacing. XSW is unable to distinguish layer spacings which differ by an integral number of bulk layer spacings and the experimental value is always referenced to the nearest extended bulk scatterer plane below. To overcome this ambiguity one must always consider the consequences of adding one or two bulk layer spacings to the experimental value in order to determine the correct structure; incorrect solutions are usually easily rejected as leading to adsorbate-substrate nearest-neighbour distances which fall well outside the range of acceptability. In the case of the pure Cl and Rb layers on Cu(111) these arguments have already been discussed at length elsewhere [16, 17, 23]. Despite the good fit of the coherent positions in the site triangulation for both species, the $(\bar{1}11)$ coherent fractions are substantially less than unity, implying, at the very least, substantial disorder. In the case of the (2 × 2)-Rb phase this low coherent fraction was also found in the original study [23]; one possible origin is large vibrational amplitudes parallel to the surface which have been postulated in other studies of atop geometries for alkalis on fcc (111) surfaces [21, 25], although the very low value in the case of Cu(111)/Rb is apparently not easily improved by cooling [23]. For our present purposes we need only note, however, that these (2 × 2)-Rb-phase NIXSW are in good agreement with the previous study. The $(\bar{1}11)$ coherent fraction for the ($\sqrt{3} \times \sqrt{3}$)R30°-Cl phase, while not so low as that for the (2 × 2)-Rb phase, is still significantly smaller than one might expect for occupation of a single adsorption site. The earlier NIXSW study of this structure [16, 17] involved measurement of only the (111) reflection and so cannot be compared, although scanned-energy-mode photoelectron diffraction data did indicate occupation of the fcc hollow alone [26, 27]. A further relevant comparison is with a full NIXSW investigation of a mixed Cl/Br adsorption phase, also with average ($\sqrt{3} \times \sqrt{3}$) periodicity, produced by dissociation of 1-bromo-2-chloroethane on Cu(111)

[28]. In this case the data gave even lower $(\bar{1}11)$ NIXSW coherent fractions than for the pure Cl phase studied here and these were interpreted as being consistent with mixed hollow-site occupation, with some 25% of hcp sites being occupied. It is possible that a smaller partial fraction of hcp site occupation may account for the present data on the pure Cl phase. Again, this issue is not really germane to the main subject of this paper as we shall see that the coadsorption produces a massive reordering of the Cl overlayer, so its original state of order is probably not particularly relevant.

Turning now to the NIXSW results for the coadsorbed phase it is immediately obvious from table 1 that there is, indeed, a significant site change for the Cl atoms. The Cl absorber coherent positions are quite different from their original values prior to the Rb coadsorption.

For the coadsorbed layer the (111) coherent positions of the Rb and Cl are now very similar, while the $(\bar{1}11)$ coherent fractions for both absorbers are now very low (with values whose differences from zero are only marginally significant). There are also significant reductions of the (111) coherent fractions from the rather high values of both of the pure layers. The fact that the Rb and Cl(111) coherent positions are very similar suggests a coplanar coadsorbed layer and thus encourages us to consider models based on the geometry of bulk RbCl. In this regard we should note that the TPD results for this system [12] also suggest compound formation.

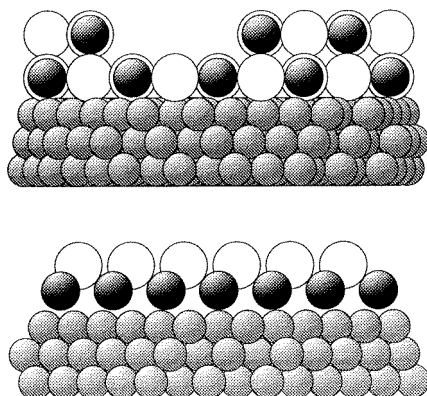


Figure 2. A sectional view of the two alternative models for RbCl growth on Cu(111). In both figures the smallest light-shaded balls represent three outermost layers of the Cu(111) substrate, while the larger open balls (Cl) and dark-shaded balls (Rb) of the RbCl overlayer are drawn with their ionic radii. (a) shows a complete first layer and partial second layer of RbCl(100), while (b) shows a complete double layer of RbCl(111). The overlayer–substrate registry is arbitrary, as is the ordering of the Rb and Cl layers in the polar RbCl(111) double layer.

To evaluate the idea of a RbCl overlayer we first consider the consequences of different possible geometries. Our starting point in the formation of the coadsorbed layer is the $(\sqrt{3} \times \sqrt{3})R30^\circ$ -Cl layer with a nominal coverage of 0.33 ML corresponding to 5.93×10^{18} Cl atoms per m^2 . Of course, 0.33 ML would be a fully saturated surface, so it is probable that the true coverage is less than this, perhaps by 5–10%. To this surface we have added Rb ‘to saturation’ which, for stoichiometric RbCl, would imply the same coverage of Rb atoms. Consider, now, possible bulk RbCl orientations. The orientation which would match the substrate symmetry is (111), but this is a polar surface with alternate layers of pure Rb and pure Cl. The atom density in each of these layers is $5.41 \times 10^{18} \text{ m}^{-2}$, slightly less than the nominal 0.33 ML Rb and Cl coverage, so if the overlayer were to have

the structure of RbCl(111), then after allowance for a probable coverage shortfall of 5–10% for the nominal 0.33 ML it should comprise almost exactly one complete double layer. The double-layer spacing in bulk RbCl is 1.90 Å, not radically different from the bulk Cu(111) layer spacing (2.08 Å), so a double layer would lead to very similar Rb and Cl(111) coherent positions, with the upper layer being referenced to the next extended bulk scatterer plane. On the other hand, this double layer would have a large dipole moment perpendicular to the surface and might therefore be expected to be energetically unfavourable. By contrast, the lowest-energy surfaces of the alkali halides (the cleavage faces) are (100) which are non-polar. In the case of RbCl, a single layer of (100) comprises $4.62 \times 10^{18} \text{ m}^{-2}$ of Rb atoms and the same density of coplanar Cl atoms. A RbCl(100) overlayer containing the original 0.33 ML of Cl and Rb atoms would then comprise 1.28 layers of the compound, with a layer separation (of bulk RbCl(100) planes) of 3.29 Å. Figure 2 shows these two models schematically.

In order to determine the consequences of these two structural models for a NIXSW experiment it is necessary to understand the relationship between actual layer spacings and measured coherent positions and fractions when more than one site is occupied. To do so it is helpful to write down in its complex form the general equation relating the measured coherent position, D , and coherent fraction, f_{co} , to the actual distribution of adsorbate layer spacings $f(z)$ where z is measured relative to the appropriate Bragg scattering planes (defined by the crystallographic indices H) whose spacing is d_H :

$$f_{co} \exp(2\pi i D/d_H) = \int_0^{d_H} f(z) \exp(2\pi i z/d_H) dz. \quad (1)$$

An important attraction of this formulation is that one can use it to construct a simple graphical representation of the way in which the measured quantities f_{co} and D relate to the integral over the real spatial distribution function. This is achieved using an Argand diagram—each layer spacing in the spatial distribution is represented by a vector, the direction being defined by the phase angle $2\pi z/d_H$ relative to the positive x -axis, while the length is $f(z)$ which is the probability of this value; the resultant (the vector sum of these components) is a vector of length f_{co} and phase angle $2\pi D/d_H$ [24]. One rather direct result obtained from this formulation which is of especial interest to the present discussion is the consequence of having two different adsorbate layer spacings which differ by one half of the substrate layer spacing. In this case the two vectors representing these sites on the Argand diagram have phase angles which differ by exactly π ; the two vectors are therefore opposed, and the resultant, for equal occupation of the two sites (equal lengths of the individual vectors), is zero—i.e. a coherent fraction of zero (and a coherent position which is meaningless—a vector of zero length has no phase angle!) If the occupation of the two sites is not equal, then the resultant vector will have the direction (and thus phase angle and coherent position) of the dominant site, but will have a length (coherent fraction) which is much reduced by cancellation with the opposing vector.

This particular situation almost exactly describes the consequences of the partial occupation of the second RbCl layer in the (100) model, because the RbCl(100) layer spacing value is 1.58 times that of the Cu(111) substrate and thus of the standing-wave periodicity. Because integral values of the layer spacing have no consequence, this value of 1.58 is equivalent to 0.58—close to the 0.5 value for exact cancellation. Assuming exact cancellation illustrates the consequences rather directly. If we have one complete first layer of RbCl(100) and 0.28 of the second layer, then the Argand diagram vector for the first layer will have a length of 0.78 ($=1/1.28$) and that for the second layer will have a length of 0.22 ($=0.28/1.28$); this is because $f(z)$ must be normalized to unity summed over all

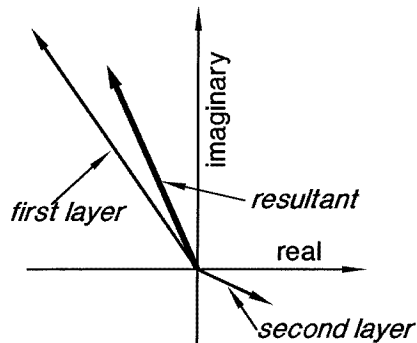


Figure 3. An illustration of the Argand diagram representing Cu(111) XSW parameters from a complete monolayer of RbCl(100) and 28% of a second layer of the same structure, as discussed in the text. The angle between the first- and second-layer vectors is $0.58 \times 2\pi$ radians, corresponding to the RbCl interlayer spacing which is 1.58 times that of the Cu(111) substrate.

sites. With exact cancellation, the resultant vector has a length of 0.56. Thus the presence of the partial second layer reduces the (111) coherent fraction for both Rb and Cl in a perfect rigid overlayer structure to 0.56. This value is changed rather little by the deviation of the layer spacing difference from exactly 1.50 substrate layer spacings (see figure 3).

This second-layer cancellation provides a clear rationale for the reduced (111) coherent fractions seen in table 1. The actual coherent fraction observed for the Rb(111) NIXSW is 0.72 rather than the value of 0.56 which we have just estimated, but this is a worst-case estimate, because it assumes that the initial Cl coverage is the maximum possible value of 0.33 ML and that all of this Cl is titrated by the Rb. If we assume a true coverage some 10% lower, then we should have 1.16 layers of RbCl and the cancellation with the actual layer spacings gives a predicted coherent fraction of 0.74. Bearing in mind the slight anticipated reduction of this value due to thermal vibrations and some disorder (typically about a 10% effect—although the thermal vibrations in the substrate account for only 3%), and also the error estimate of our experiment, it is clear that this model provides an excellent description of the Rb(111) coherent fraction in the coadsorption phase. By contrast, if the RbCl overlayer had the (111) orientation, Rb and Cl layers would be separate and the coverage should not involve a second double layer. Moreover, even if a second double layer were to be occupied, the (111) layer spacing is similar to that of the Cu substrate and thus fails to cause strong cancellation as in the (100) case. A (111) RbCl overlayer would therefore not be expected to lead to reduced (111) coherent fractions. Notice too, that for the RbCl(100) overlayer model we can exclude the possibility of multilayer islands which would cause a much more serious reduction of the coherent fractions than is actually observed.

This model of a RbCl(100) overlayer with partial occupation of a second layer accounts for the very similar (111) coherent positions for Rb and Cl (we would expect them to be identical) and accounts for the value of the (111) coherent fraction for the Rb XSW. Two further experimental observations need to be accounted for. The first of these is that the Cl (111) coherent fraction is actually significantly lower than that for the Rb absorbers. A very plausible explanation for this is that a small fraction of the Cl atoms are not titrated by the nominal saturation dose of Rb and retain their fcc hollow sites. Notice that the (111) coherent position in the pure chemisorbed Cl layer (1.81 Å) and in the coadsorbed

layer (2.81 Å for the Rb which presumably is all in the compound) differ by almost exactly half of the bulk Cu(111) layer spacing (1.00 Å compared with 1.04 Å), again providing the condition leading to a lowering of the coherent fraction with no significant change in the coherent position. The second question concerns the $(\bar{1}11)$ XSW parameters for both the Rb and Cl absorbers in the coadsorption state. If we have a true bulk-structure RbCl(100) overlayer, this should be incommensurate with the substrate, leading to zero coherent fraction for any XSW which has its nodal planes not parallel to the surface [24]. In such a situation, as we have already remarked, the coherent positions become meaningless. Our data come close to this prediction. The best fits to the $(\bar{1}11)$ NIXSW absorption profiles do indicate a non-zero coherent fraction, but the difference between the measured value and the predicted zero is only marginally significant. One possibility is that the RbCl overlayer is broken up into smaller islands, separated by anti-phase domain boundaries. In such a situation, it is possible that the atop geometry for the overlayer atoms implied by the (111) and $(\bar{1}11)$ coherent positions is marginally favoured. In this context we should note that for an overlayer species which fails to distinguish the fcc and hcp hollow sites on an fcc (111) surface, adsorbate positions within large areas of the surface (outside the true high-symmetry atop sites) can be shown to have (111) and $(\bar{1}11)$ coherent positions indicative of atop sites [29].

4. Summary and conclusions

Our NIXSW study of the results of adsorbing Rb to nominal saturation on a Cu(111)($\sqrt{3} \times \sqrt{3}$)R30°-Cl surface are consistent with the formation of an overlayer of RbCl(100) with partial (about 15%) occupation of a second layer, as required by the coverage, but exclude the possibility of multilayer islands. This orientation of the RbCl compound is favoured over the alternative (111), which has the same symmetry as the substrate, not only because this orientation (which would produce a highly polar double layer) is likely to be energetically unfavourable, but also because this model does not fit the measured coherent fractions as well. Other possible orientations of RbCl have not been considered. The formation of the RbCl compound is also suggested by the results of the prior TPD study [12] which indicates desorption of both Rb and Cl in a concerted reaction at a temperature which differs from that found for either species alone. One further experimental result of relevance to these conclusions concerns an STM study of NaCl deposited on Al(111) at low coverages (less than 1 ML) [13]. The results of this study show islands of an overlayer with an atomic-scale periodicity consistent with NaCl(100), and indicate island thicknesses which are probably a single monolayer. Interestingly, these overlayer islands can easily be moved over the surface by the tip, and are seen to form ‘carpets’ which may continue over surface steps in the substrate. Both effects suggest strong adsorbate–adsorbate coupling within the overlayer, and very little corrugation of the adsorbate–substrate potential, a conclusion consistent with an incommensurate overlayer. These STM studies also indicate that the NaCl overlayer can be destroyed by energetic electrons, produced by raising the tunnelling bias, a conclusion qualitatively consistent with the sensitivity of our RbCl overlayer to ESD by electrons in the LEED energy range [12].

Acknowledgments

The authors are pleased to acknowledge the support of the Science and Engineering Research Council in the form of synchrotron radiation beamtime on the SRS and a studentship for

one of us (GJ), and of the European Commission through a Network grant under the Human Capital and Mobility Programme (grant No ERBCHRXCT940571).

References

- [1] See, e.g.,
King D A and Woodruff D P (ed) 1993 *Coadsorption, Promoters and Poisons (The Chemical Physics of Solid Surfaces 6)* (Amsterdam: Elsevier)
- [2] Davis R, Woodruff D P, Schaff O, Fernandez V, Schindler K-M, Hofmann P, Weiss K-U, Dippel R, Fritzsche V and Bradshaw A M 1995 *Phys. Rev. Lett.* **74** 1621
- [3] Over H, Bludau H, Kose R and Ertl G 1995 *Phys. Rev. B* **51** 4661
- [4] Kaukasoina P, Lindroos M, Hu P, King D A and Barnes C J 1995 *Phys. Rev. B* **51** 17 063
- [5] Scragg G, Kerkar M, Ettema A R H F, Woodruff D P, Cowie B C C, Daimellah A, Turton S and Jones R G 1995 *Surf. Sci.* **328** L533
- [6] Scragg G, Kerkar M, Ettema A R H F, Woodruff D P, Cowie B C C, Daimellah A, Turton S and Jones R G 1995 *J. Chem. Soc. Faraday Trans.* **91** 3555
- [7] Over H, Bludau H, Skottkeklein M, Moritz W and Ertl G 1992 *Phys. Rev. B* **46** 4360
- [8] Bowker M, Wolindale B, King D A and Lamble G 1987 *Surf. Sci.* **192** 95
- [9] Souda R, Hayami W, Aizawa T, Otani S and Ishizawa Y 1993 *J. Vac. Sci. Technol. A* **11** 535
- [10] Jaegermann W and Mayer T 1995 *Surf. Sci.* **335** 343
- [11] Namiki A, Ukai Y, Hayashi H, Nakamura T and Geuzebroek F H 1995 *Surf. Sci.* **337** 8
- [12] Spiros S and Papageorgopoulos C A 1997 to be published
- [13] Hebenstreit W, Horosova S, Schmidt M and Varga P 1997 to be published
- [14] MacDowell A A, Norman D, West J B, Campuzano J C and Jones R G 1986 *Nucl. Instrum. Methods A* **246** 131
- [15] MacDowell A A, Norman D and West J B 1986 *Rev. Sci. Instrum.* **57** 2667
- [16] Woodruff D P, Seymour D L, McConville C F, Riley C E, Crapper M D, Prince N P and Jones R G 1987 *Phys. Rev. Lett.* **58** 1460
- [17] Woodruff D P, Seymour D L, McConville C F, Riley C E, Crapper M D, Prince N P and Jones R G 1988 *Surf. Sci.* **195** 237
- [18] Walter W K and Jones R G 1992 *Surf. Sci.* **264** 391
- [19] Walter W K, Jones R G, Waugh K C and Bailey S 1994 *Catal. Lett.* **24** 33
- [20] Jones R G, Turton S and Ithnin R 1996 *Chem. Phys. Lett.* **261** 539
- [21] Kerkar M, Fisher D, Woodruff D P, Jones R G, Diehl R D and Cowie B 1992 *Phys. Rev. Lett.* **68** 3204
- [22] Kerkar M, Hayden A B, Woodruff D P, Kadodwala M and Jones R G 1992 *J. Phys.: Condens. Matter* **4** 5043
- [23] Heskett D, Xu P, Berman L, Kao C C and Bedzyk M J 1995 *Surf. Sci.* **344** 267
- [24] Woodruff D P, Cowie B C C and Ettema A R H F 1994 *J. Phys.: Condens. Matter* **6** 10 633
- [25] Davis R, Hu X M, Woodruff D P, Weiss K U, Dippel R, Schindler K-M, Hofmann P, Fritzsche V and Bradshaw A M 1994 *Surf. Sci.* **307-309** 632
- [26] Crapper M D, Riley C E, Sweeney P J J, McConville C F, Woodruff D P and Jones R G 1986 *Europhys. Lett.* **2** 857
- [27] Crapper M D, Riley C E, Sweeney P J J, McConville C F, Woodruff D P and Jones R G 1987 *Surf. Sci.* **182** 213
- [28] Kadodwala M F, Davis A A, Scragg G, Cowie B C C, Kerkar M, Woodruff D P and Jones R G 1995 *Surf. Sci.* **324** 122
- [29] Jackson G J, Lüdecke J, Driver S M, Woodruff D P, Jones R G, Chan A and Cowie B C C 1997 *Surf. Sci.* submitted